AEDC-TN-61-66

Unclassified

INVESTIGATION OF BOUNDARY-LAYER SUCTION ON A 20-CALIBER OGIVE CYLINDER AT MACH NUMBERS 2.5, 3.0, 3.5, AND 4.0

By
W. T. Strike and S. Pate
VKF, ARO, Inc.

June 1961

ARNOLD ENGINEERING DEVELOPMENT CENTER

AIR FORCE SYSTEMS COMMAND

U S A F

Unclassified

INVESTIGATION OF BOUNDARY-LAYER SUCTION ON A 20-CALIBER OGIVE CYLINDER AT MACH NUMBERS 2.5, 3.0, 3.5, AND 4.0

By

W. T. Strike and S. Pate

VKF, ARO, Inc.

June 1961

ARO Project No. 311128
Program Area 750A, Project No. 1366, Task No. 14080

Contract No. AF 40(600)-800 S/A 11(60-110)

ABSTRACT

A second investigation was conducted in the 12-in., intermittent, supersonic wind tunnel of the von Kármán Gas Dynamics Facility to measure the effectiveness of boundary-layer suction on a 20-caliber ogive cylinder. The application of suction-type boundary-layer control on the ogive was investigated at Mach numbers 2.5, 3.0, 3.5, and 4.0 over a unit Reynolds number range from 0.07 to 1.03×10^6 per inch with the model at zero angle of attack. Some additional data were obtained at 2-deg angle of attack at Mach number 3. As a result of improving the design of the suction system a significant gain was made in reducing the net drag of the model at Mach number 3 by boundary-layer suction. The presence of the suction slots with no suction when compared with the sealed slot configuration (that is, smooth model) had some influence on the boundary-layer characteristics at all Mach numbers.

CONTENTS

ILLUSTRATIONS

NOMENCLATURE

A_b	Model base area, 8.296 sq in.
A_w	Model wetted area, 144 sq in. up to model station, 18.8 in.
C_{D_F}	Frictional-drag coefficient, $2\epsilon \left(\frac{A_b}{A_w}\right)$
C_{D_S}	Suction-drag coefficient, $\dot{m} U_\infty / q_\infty A_w$
C_m	Suction mass-flow coefficient, $\dot{m}/\rho_\infty U_\infty A_w$
D_F	Frictional drag, lb
D_S	Suction drag, lb
M_∞	Free-stream Mach number
$\dot{m}$	Mass rate of suction, lb-sec/in.
p	Local model static pressure, psia
p_t	Local model pitot pressure, psia
q_∞	Free-stream dynamic pressure, psia
Re	Reynolds number, based on distance to rake location
r_m	Maximum model radius, 1.625 in.
U	Local velocity in boundary layer, in./sec
U_ℓ	Local velocity outside boundary layer, in./sec
U_∞	Free-stream velocity, in./sec
x	Model axial position, in.
x_t	Boundary-layer transition location, in.
y	Distance normal to model surface, in.
α	Angle of attack, deg
Δ^*	Boundary-layer displacement parameter, in., $r_m \int_0^\delta \left(1 - \left(\frac{\rho U}{\rho_\ell U_\ell}\right)\right) d\left\{\frac{y}{r_m} + \frac{1}{2}\left(\frac{y}{r_m}\right)^2\right\}$
δ	Boundary-layer total thickness, in.
δ^*	Boundary-layer displacement thickness, in., $(\rho_\ell U_\ell / \rho_\infty U_\infty)\Delta^*$
ϵ	Boundary-layer momentum loss coefficient, $2(\theta/r_m)$

θ Boundary-layer momentum thickness, in.,

$$(\rho_\ell \, U_\ell^2/\rho_\infty \, U_\infty^2)\,\theta^*$$

θ^* Boundary-layer momentum parameter, in.,

$$r_m \int_0^\delta \frac{\rho \, U}{\rho_\ell \, U_\ell} \left(1 - \frac{U}{U_\ell}\right) d\left\{\frac{y}{r_m} + \frac{1}{2}\left(\frac{y}{r_m}\right)^2\right\}$$

ρ Local density in the boundary layer, lb-sec^2/in.^{4}

ρ_ℓ Local density outside the boundary layer, lb-sec^2/in.^{4}

ρ_∞ Free-stream density, lb-sec^2/in.^{4}

ϕ Radial coordinate angle from leeward side, deg

INTRODUCTION

An experimental program utilizing boundary-layer suction to delay transition on a body of revolution was investigated for the NORAIR Division of the Northrop Corporation under the sponsorship of Aeronautical Systems Division (ASD) in the 12-in., intermittent, supersonic tunnel (Tunnel E-1) of the von Kármán Gas Dynamics Facility (VKF), Arnold Center (AFSC). An earlier test program* utilizing a 20-caliber ogive cylinder was conducted for NORAIR at Mach numbers 2.5, 3.0, and 3.5 in Tunnel E-1 in May 1958, but because of suction flow limitations resulting primarily from the model design only limited suction results were obtained. Using the same configuration and model size, the NORAIR Division increased the number of suction slots and the internal suction line diameters to reduce the pressure drop through the suction system and thus improve the performance of the model.

The primary purpose of the present program was to evaluate the effects of boundary-layer suction on the improved model. The test was conducted during the period from February 13 through March 3, 1961. Test results were obtained at Mach numbers 2.5, 3.0, 3.5, and 4.0 at an overall Reynolds number range from 0.07 to 1.03 million per inch. At Mach number 3, the effectiveness of boundary-layer suction was measured at 2-deg angle of attack and at zero angle of attack at Mach numbers 2.5, 3.0, 3.5, and 4.0.

APPARATUS

WIND TUNNEL

Tunnel E-1 is an intermittent, supersonic wind tunnel with a 12-in. by 12-in. test section (Fig. 1). The top and bottom walls of the nozzle are flexible plates which are positioned by screw jacks to vary the Mach number within the range from 1.5 to 5. The maximum allowable stress on the flexible nozzle plate limits the tunnel supply pressure to a maximum of four atmospheres, which is maintained by throttling the flow from a surface-heated, high-pressure, air storage system. A large vacuum sphere coupled to the downstream end of the tunnel permits operation at low density levels.

Manuscript released by authors May 1961.

*W. T. Strike and J. C. Donaldson. "Investigation of Suction Controlled Boundary Layer on a Northrop Model at Mach Numbers of 2.5, 3.0, and 3.5." AEDC-TN-59-80, July 1959.

MODEL

A 20-caliber, tangent, ogive cylinder (Figs. 2 and 3) was used as a typical body of revolution. The model, approximately seven calibers long with a 3.25-in. base diameter, was strut-mounted to the tunnel floor. Four, surface, static pressure orifices were located at various model stations (Fig. 2). The model with four independent, internal suction chambers was fabricated with separate inner and outer shells. A shrink fit process was used to hold the two shells in place. The outer shell consisted of contoured aluminum bands separated by spaces which formed slots (0.004 to 0.006 inches in width) over rings of holes in the inner shell (Fig. 4). Thus, with suction applied air flowed through the slot into a small plenum chamber between the inner and outer shells and then through the holes of the inner shell into a suction chamber. The model, the suction metering boxes, a common suction tank, and associated suction lines were furnished by NORAIR.

A boundary layer rake (Fig. 3) consisting of seven total head probes made of 0.016-in. O.D. steel tubes was mounted on the model. The rake could be positioned at any station along the cylindrical portion of the model.

SUCTION SYSTEM

A schematic of the suction system is outlined in Fig. 4. From each of the four model suction chambers, a suction line was connected to a metering box, containing a throttle valve and an interchangeable converging nozzle, which was used to regulate and measure the mass of air removed from the boundary layer. Four evacuating lines from the metering boxes were connected to a common 12-in.-diam suction line.

INSTRUMENTATION

All pressures were measured with differential transducers using a reference pressure of 10 to 80 microns of mercury. The reference pressures were measured by low-pressure gages and incorporated in the data reduction program. The output of the transducers and thermocouples was monitored on self-balancing potentiometers which were digitized so that data could be automatically recorded, computed, and tabulated.

Aside from the tunnel test conditions, the following information was recorded during the test: four model surface static pressures, model

suction chamber pressures and temperatures, metering chamber stagnation pressures and temperatures, and the differential pressure between stagnation and nozzle static pressure of each of the metering boxes.

A conservative estimate of the precision of this data at Mach number 3 in terms of the pressure ratio (p/p_t) was ±0.4 percent which resulted in a velocity ratio (U/U_ℓ) reliability of ±0.2 percent. It was not feasible to obtain a true statistical estimate of the uncertainty of the boundary-layer parameters because these computations depended upon the fairing of curves, the accuracy of the measurements of the rake geometry, and the use of a planimeter to graphically integrate the momentum and displacement parameter distributions.

Shadowgraph pictures of the flow on the model in the region ahead of the boundary-layer rake were taken for nearly all test points.

PROCEDURE

The tests were conducted in Tunnel E-1 at the following test conditions:

Nominal Mach No.	Mach No.	Re/in. x 10^6	Boundary-Layer Rake Locations, in.	
2.5	2.50	≈ 0.10 to 1.03	18.8	With or Without Suction
3.0	3.00	≈ 0.07 to 0.84	18.8	
3.5	3.49	≈ 0.10 to 0.60	19.1	With Suction
4.0	3.98	≈ 0.08 to 0.46	19.1	

Except for some test results at Mach number 3, the boundary-layer profiles were measured with the model at zero angle of attack at each Mach number. At Mach number 3 some measurements were obtained with the model at 2-deg angle of attack.

The test procedure consisted of first determining the stagnation pressure at which transition occurred at the boundary-layer rake without suction by noting the rate of change of the local pitot pressures with free-stream stagnation pressures. Starting with the conditions where the boundary layer was turbulent at the rake, the effects of suction were determined for various free-stream Reynolds numbers.

After the suction phase of testing, the boundary-layer profile was measured at each Mach number over the maximum available Reynolds number range with no suction when the rake was placed 18.8 in. aft of the model nose. Data were obtained with the suction slots open and with the evacuating lines to the metering boxes sealed. These measurements were then repeated with the suction slots sealed by dental plaster.

DATA ANALYSIS

The experimental data were analyzed as follows. Since the measurements were performed on a body of revolution, a boundary-layer momentum loss coefficient (ϵ) was obtained by dividing the loss of the momentum in the boundary layer by the product of $\rho_\ell U_\ell^2$ and the model base area.

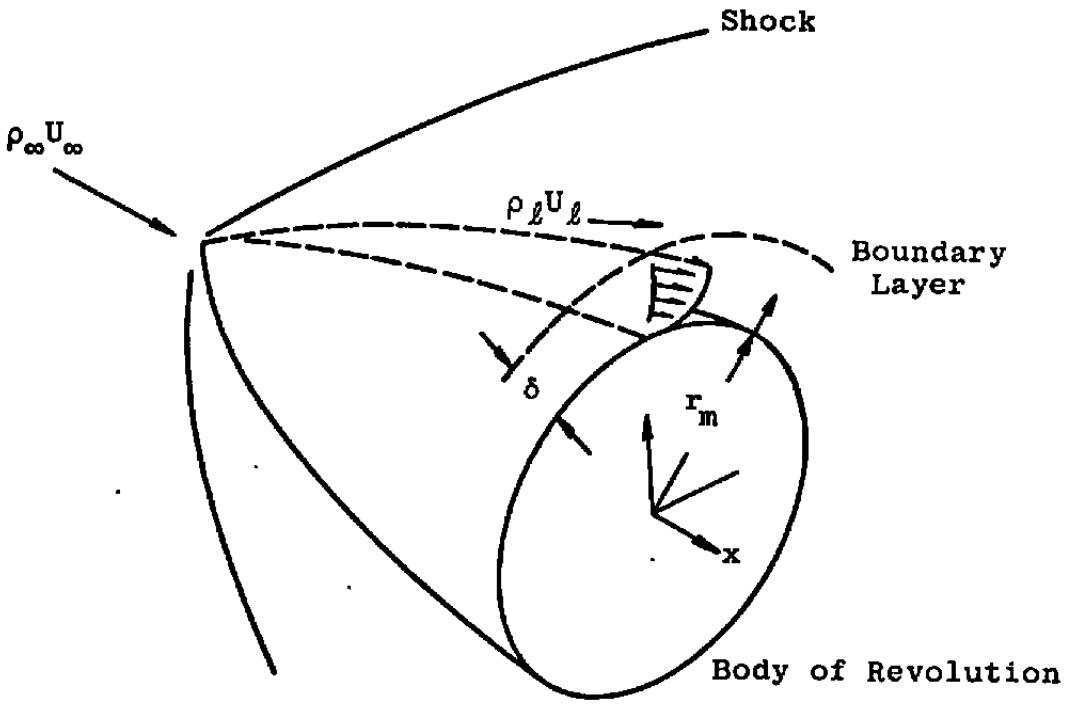

The following relations were used to define the boundary-layer momentum thickness θ, the displacement thickness δ^*, and skin-friction coefficient C_{D_F}:

$$\frac{\theta^*}{r_m} = \int_0^\delta \frac{\rho U}{\rho_\ell U_\ell}\left(1 - \frac{U}{U_\ell}\right) d\left\{\frac{y}{r_m} + \frac{1}{2}\left(\frac{y}{r_m}\right)^2\right\}$$

where $$\frac{\theta}{r_m} = \left(\frac{\rho_\ell U_\ell^2}{\rho_\infty U_\infty^2}\right)\frac{\theta^*}{r_m}$$

and $\epsilon = 2(\theta/r_m)$, $C_{D_F} = 2\epsilon\,(A_b/A_w)$

Similarly the displacement thickness was defined as

$$\Delta^*/r_m = \int_0^\delta \left(1 - \frac{\rho U}{\rho_\ell U_\ell}\right) d\left\{\frac{y}{r_m} + \frac{1}{2}\left(\frac{y}{r_m}\right)^2\right\}$$

$$\delta^*/r_m = (\rho_\ell U_\ell/\rho_\infty U_\infty)\,(\Delta^*/r_m)$$

The suction coefficient C_m was defined as $C_m = m/(\rho_\infty U_\infty A_w)$.

Assuming that all of the momentum of the air removed from the boundary layer has been lost, the corresponding minimum suction drag (D_S) is equal to the product of mU_∞. Hence the suction-drag coefficient, referred to the model wetted area, is

$$C_{D_S} = D_S/q_\infty A_w = 2C_m$$

The effectiveness of the suction at Mach number 3 was evaluated over the Reynolds number range with the ratio of the total (suction and friction) drag to the drag without suction (that is, friction drag) with the model slots sealed.

RESULTS AND DISCUSSION

Typical plots of the velocity ratio (U/U_ℓ), displacement, and momentum distribution in the boundary layer on the 20-caliber ogive cylinder at Mach number 3 over a Reynolds number range at zero angle of attack are presented in Fig. 5. These data represent the boundary-layer characteristics of a smooth, continuous, ogive surface (that is, the slots in the 20-caliber ogive cylinder were sealed with dental plaster to station 18.8). As expected, the laminar profile thickness decreased with increasing Reynolds number until the boundary layer became partially turbulent or until transition occurred in the region of the boundary-layer rake. A further increase in Reynolds number in the range between a fully laminar and turbulent boundary layer resulted in the usual increase in the boundary-layer profile thickness.

At 2-deg angle of attack the variation of the boundary-layer profiles varied around the ogive at model station 18.8 in. as shown in Fig. 6. These data were taken at Mach number 3 with the model slots open but with no suction. On the leeward side of the model (ϕ = 0 deg) the boundary-layer profiles were thickest, and transition of the boundary layer from laminar to partially turbulent flow at a free-stream Reynolds number of 0.19×10^6 per inch occurred between the windward side and the 90-deg radial position. An increase in Reynolds number to 0.84×10^6 per inch produced turbulent flow at radial positions ϕ = 0, 90, and 180 deg.

In Fig. 7, the influence of the suction slots without suction on the boundary-layer characteristics are presented for Mach numbers 2.5, 3.0, 3.5, and 4.0. In the case of the slotted model with no applied suction, some local suction and blowing will result from the axial pressure

gradient because a common model suction chamber was utilized for several model slots along the model surface (see Figs. 2 and 4). The rate of exchange of air between slots was governed by the magnitude of the pressure gradient and the pressure loss through the individual suction slots. In general, suction would tend to delay transition, whereas the discharge of air into the boundary layer and the presence of the slots would tend to promote early transition.

Apparently at Mach number 2.5 (Fig. 7a) the slots created an unfavorable condition which caused transition to occur sooner on the slotted model than on a smooth contoured surface when the slots were sealed. At the higher Mach numbers, namely 3.0, 3.5, and 4.0, the open slots tended to delay transition slightly and decrease the friction drag in the transitional Reynolds number range where the boundary layer was neither fully laminar nor fully turbulent. The magnitude of the delay in transition resulting from the open suction slots increased with the Mach number for Mach numbers of 3 or above.

Figure 8 presents the influence of suction and suction slots open and sealed on the boundary-layer profiles at Mach number 3. Figures 7b and 8 show that with the suction slots open the boundary-layer thickness was reduced, and the velocity profiles were altered by a measurable amount. Profiles are also presented in Fig. 8 to show a comparison of the boundary-layer profiles obtained with suction and without suction for the cases of open and sealed suction slots.

In Fig. 9, the suction-mass coefficient (which is herein referred to as the optimum suction coefficient) represents the amount of suction required to produce the minimum overall-drag coefficient $(C_{D_F} + C_{D_S})$ at a given free-stream Reynolds number. The test procedure consisted of first establishing the suction value which produced the minimum boundary-layer momentum thickness. At this condition data were recorded for near maximum suction, and additional data were obtained at reduced values. Although reducing the amount of suction tended to increase the boundary-layer momentum thickness, the overall-drag coefficient $(C_{D_F} + C_{D_S})$ could be reduced with a reduction in suction.

The optimum suction values and the relative reduction in overall drag (that is, frictional and suction drag) resulting from suction with respect to the frictional drag without suction are plotted against the free-stream Reynolds number at Mach number 3 in Fig. 9. Because boundary-layer suction tends to delay transition or stabilize the boundary layer, the optimum value of the overall drag (suction plus frictional drag) will approach but normally exceed the laminar frictional drag at a particular Reynolds number. Therefore in the Reynolds number range ($Re > 5 \times 10^6$ at $M_\infty = 3$)

where the boundary layer was transitional or turbulent, the maximum possible reduction in the overall drag must approach the laminar drag value. The laminar-drag coefficient value used in Fig. 9 to define the maximum possible drag reduction was obtained by extrapolating the laminar frictional drag values measured at the lower Reynolds number ($Re < 5 \times 10^6$ at $M_\infty = 3$) to the higher Reynolds number, where the boundary layer was normally transitional or turbulent.

Also included in Fig. 9 is a comparison of the present results to earlier test results obtained in Tunnel E-1 and reported in AEDC-TN-59-80. As a result of improving the design of the model (increasing the number of suction slots and diameter of the internal suction lines) transition of the boundary layer from laminar to turbulent flow was delayed, and transition occurred at a Reynolds number from 10 to 11 million instead of only 6 or 6.5 million as reported in AEDC-TN-59-80. The maximum suction coefficient C_m achieved in the previous test was 1.24×10^{-4}, which resulted in the optimum reduction in the overall drag of 27 percent at a Reynolds number of 6 or 6.5 million. In the present test the optimum suction coefficient C_m was 1.36×10^{-4} at a Reynolds number of 10.5×10^6, which resulted in a 58-percent reduction in the overall drag.

The optimum suction coefficient C_m, represented the total suction coefficient of all four model suction chambers. There was an unlimited number of combinations of suction distribution which equalled the total suction value plotted in Fig. 9 as the optimum suction value. In general, the amount of suction was equally divided among the four metering chambers for the optimum case. In some cases, increasing the suction beyond the optimum value would decrease the frictional drag but increase the overall drag ($C_{D_F} + C_{D_S}$) (see Fig. 9).

For a free-stream unit Reynolds number of 0.53×10^6 per inch, the variation of the location of transition as measured from shadowgraph pictures without suction is presented in Fig. 10. Included in the figure is the transition location attained with optimum suction and without suction at two-degrees angle of attack on the windward side at Mach number 3. Transition was delayed by ≈ 9.5 in. because of suction at Mach number 3.

CONCLUDING REMARKS

The presence of the suction slots in the model surface promoted early transition at Mach number 2.5 and delayed transition at Mach numbers 3.0, 3.5, and 4.0. A comparison of the net drag reduction at Mach number 3 with the results obtained during an earlier test on the same model configuration showed a significant improvement in the model performance which amounted to a 58-percent reduction in net drag at a Reynolds number from 10 to 11 million as compared to a 27-percent net drag reduction at a Reynolds number from 6 to 6.5 million. The design features which resulted in these performance gains consisted of improvements in the suction system and a closer spacing of the suction slots.

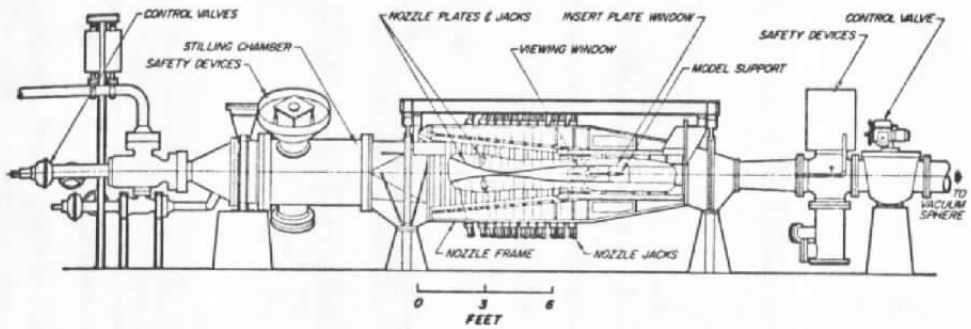

Assembly

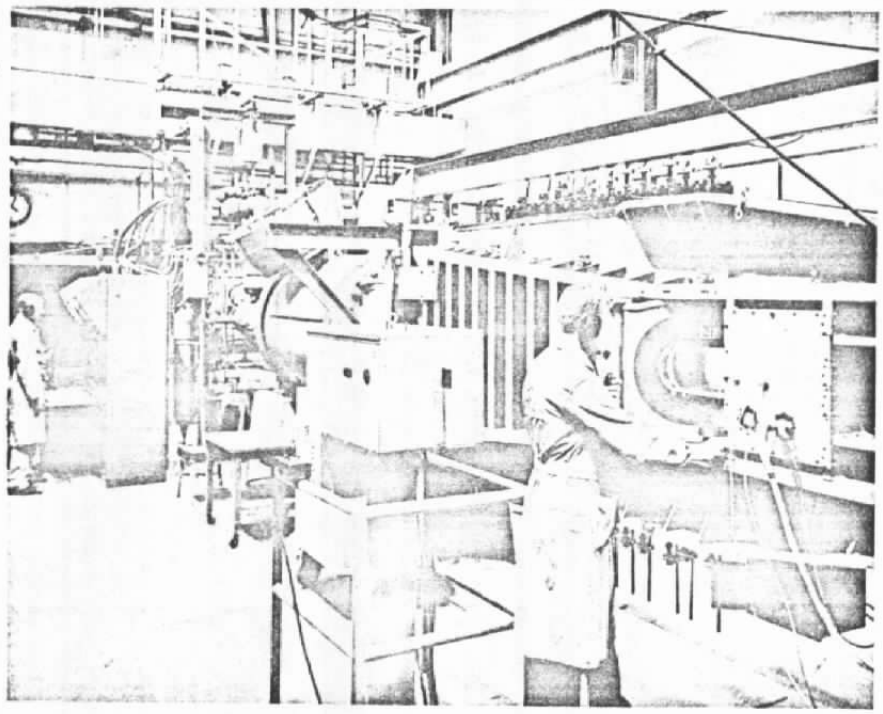

Nozzle and Test Section

Fig. 1 Tunnel E-1, a 12 x 12-in. Supersonic Wind Tunnel

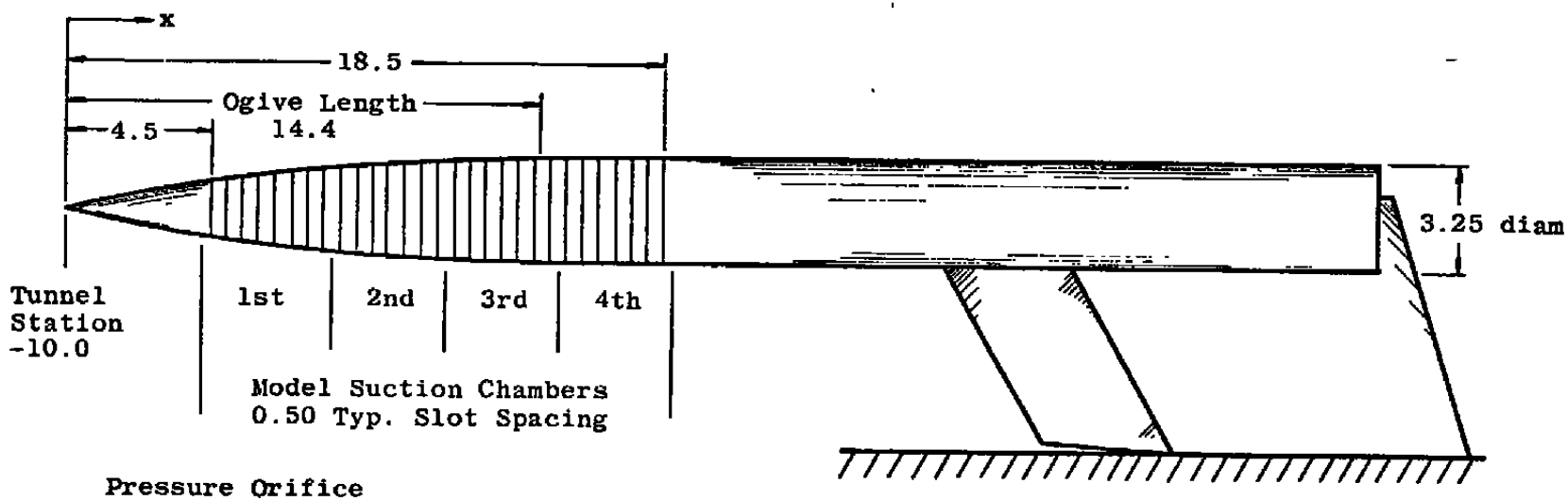

Pressure Orifice Location, x, in.

8.75
14.75
17.75
18.25

All Dimensions in Inches

Fig. 2 20-Caliber Ogive Cylinder

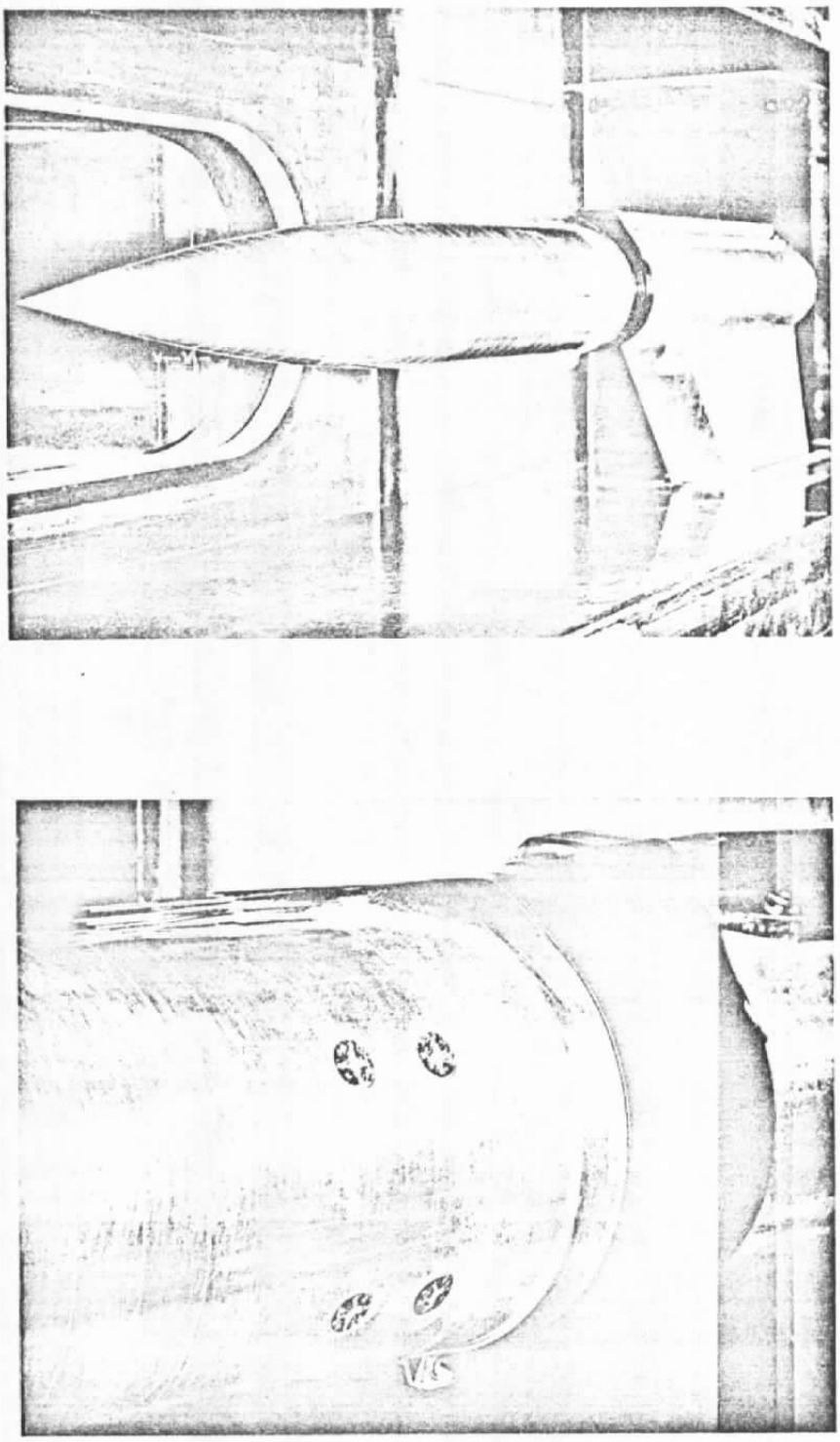

Fig. 3 Model Installation

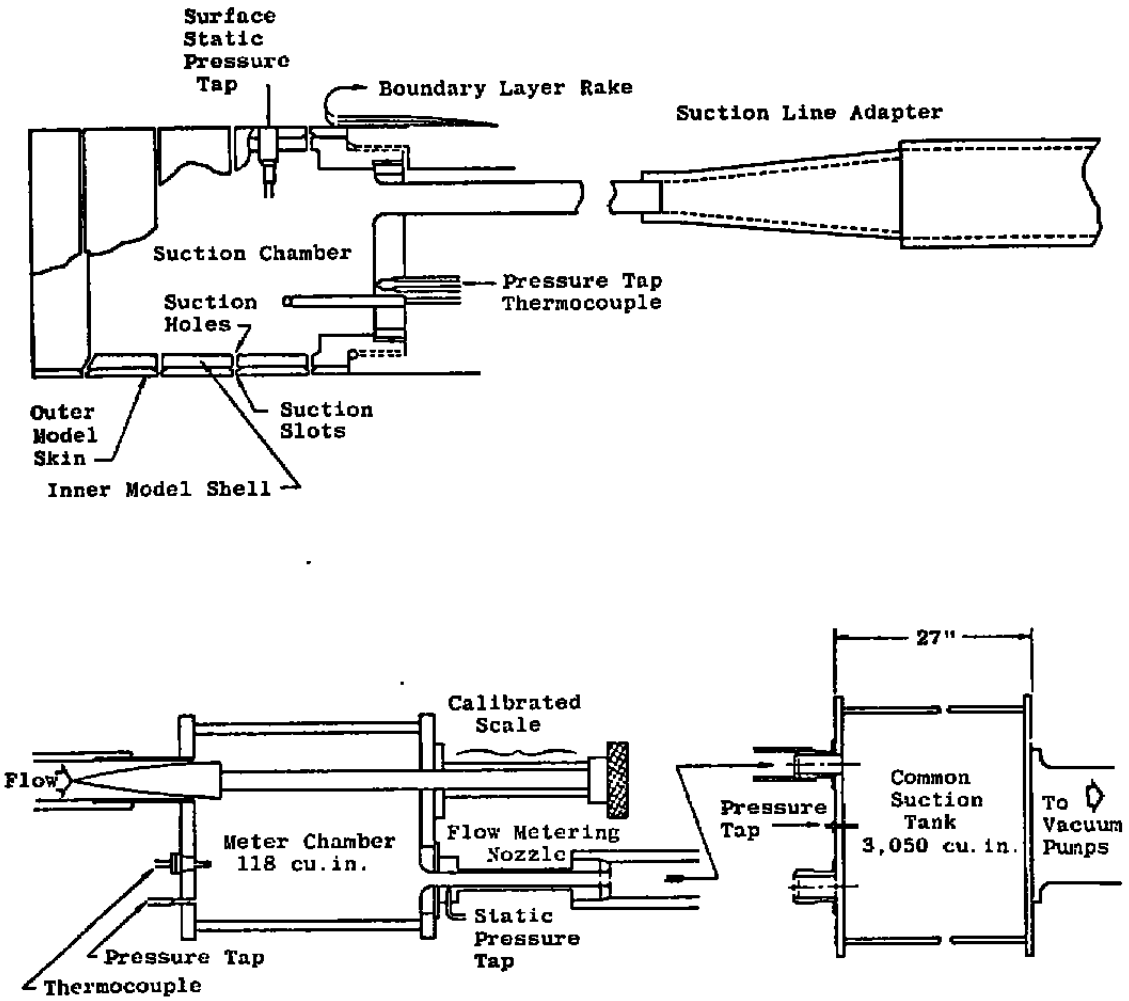

Fig. 4 Detail of Suction System

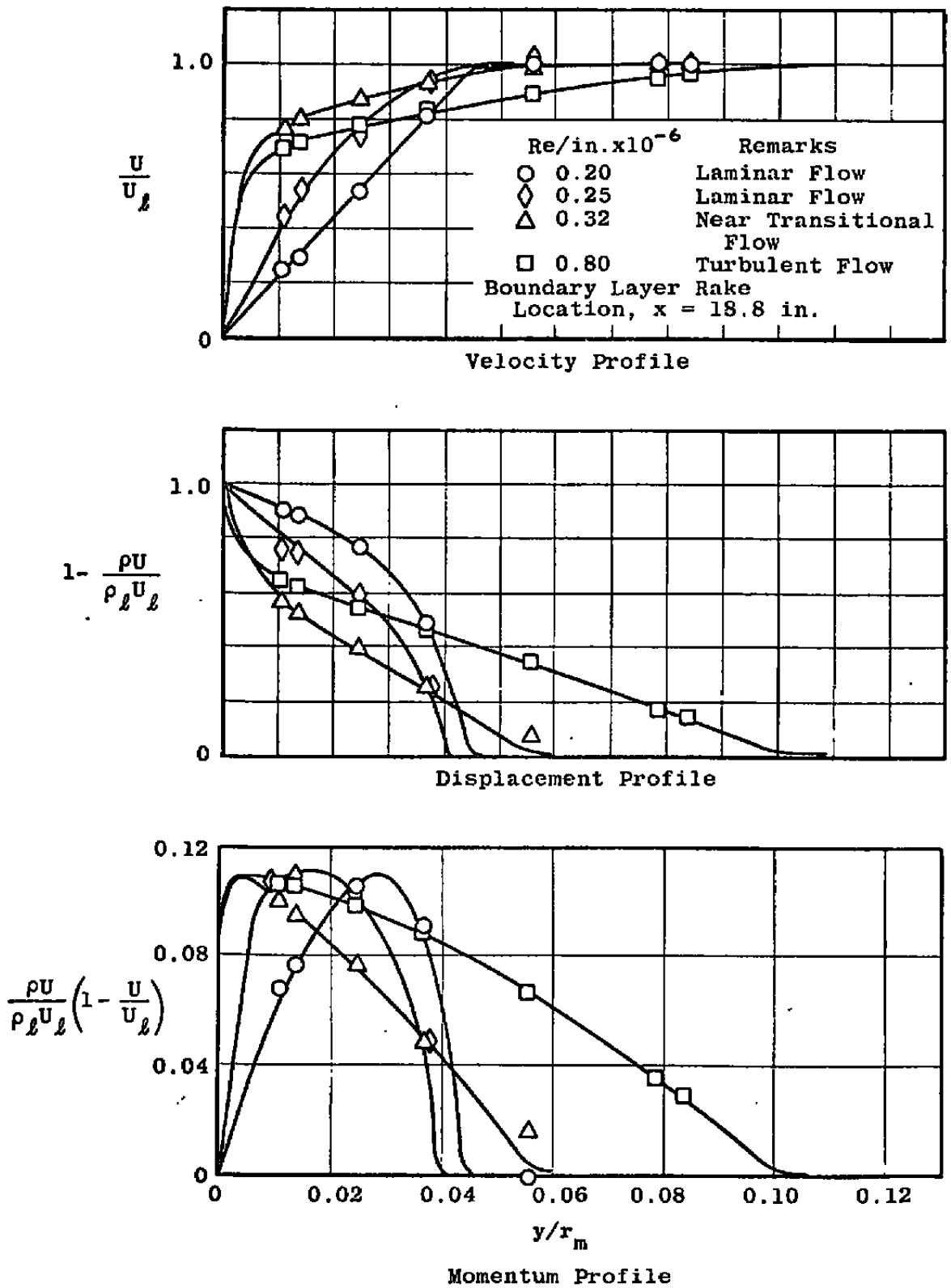

Fig. 5 Typical Boundary-Layer Profiles at Mach Number 3, $\alpha = 0$

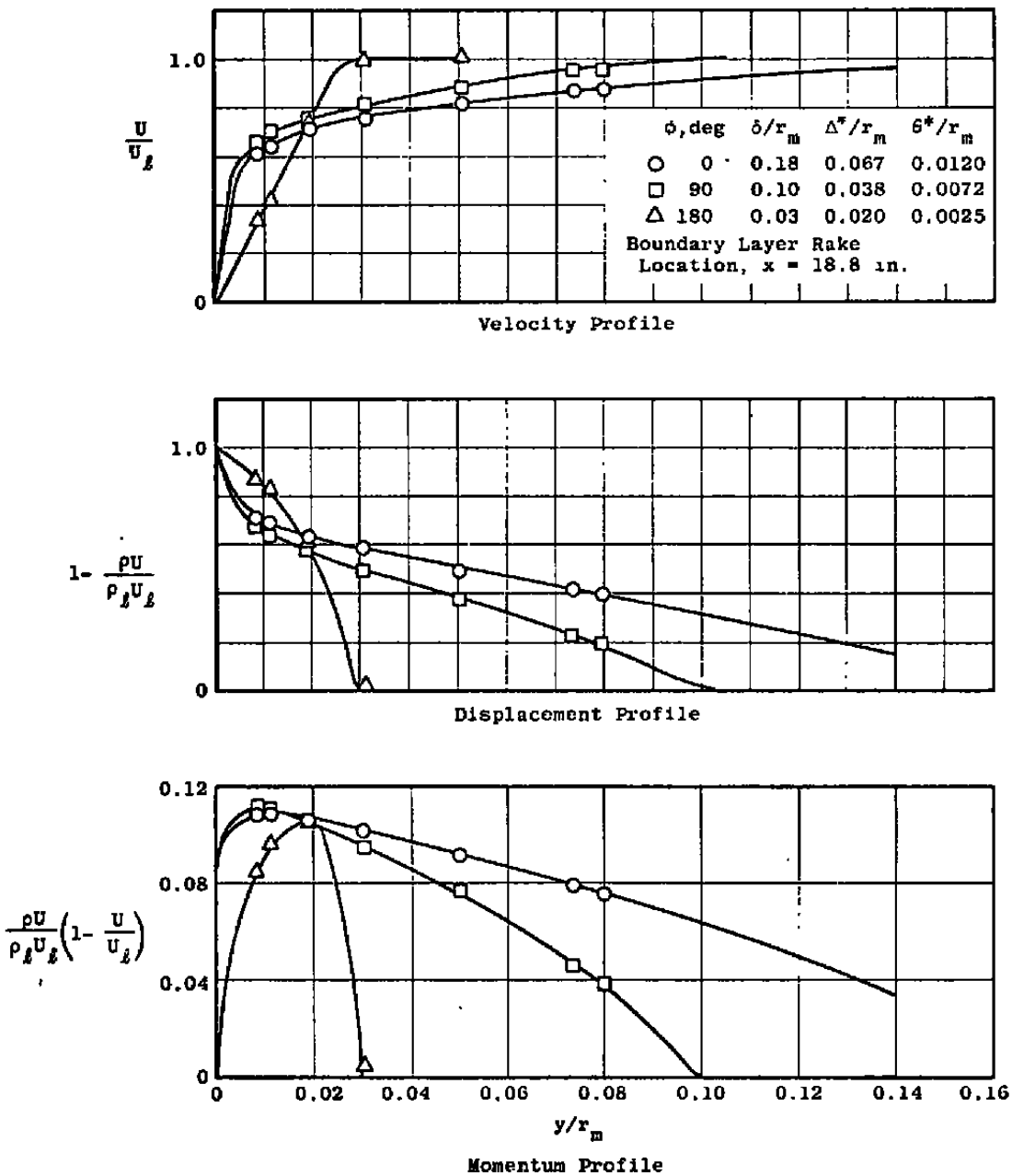

a. Re/in. = 0.19×10^6

Fig. 6 Typical Boundary-Layer Profiles at Mach Number 3, $\alpha = 2$

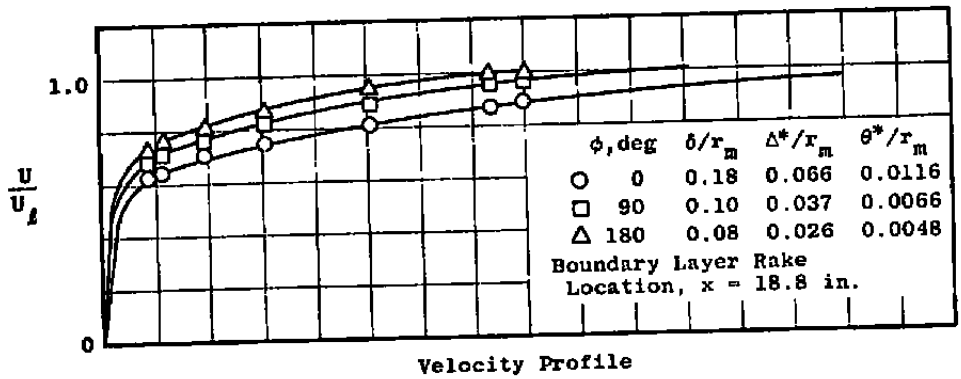

Velocity Profile

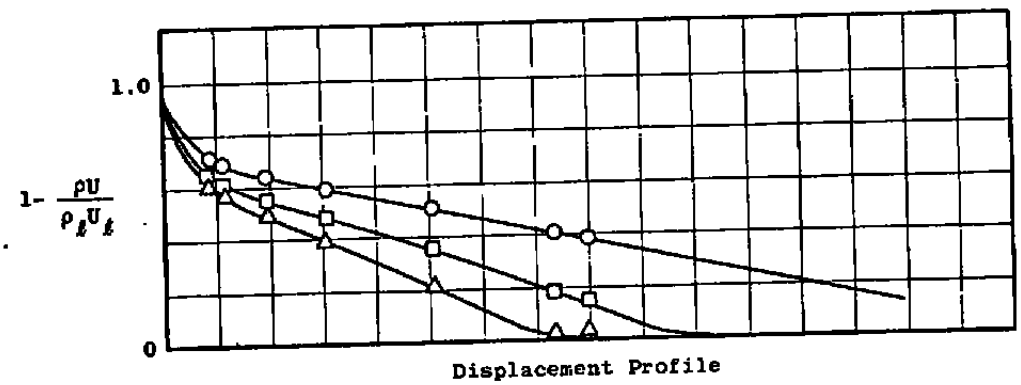

Displacement Profile

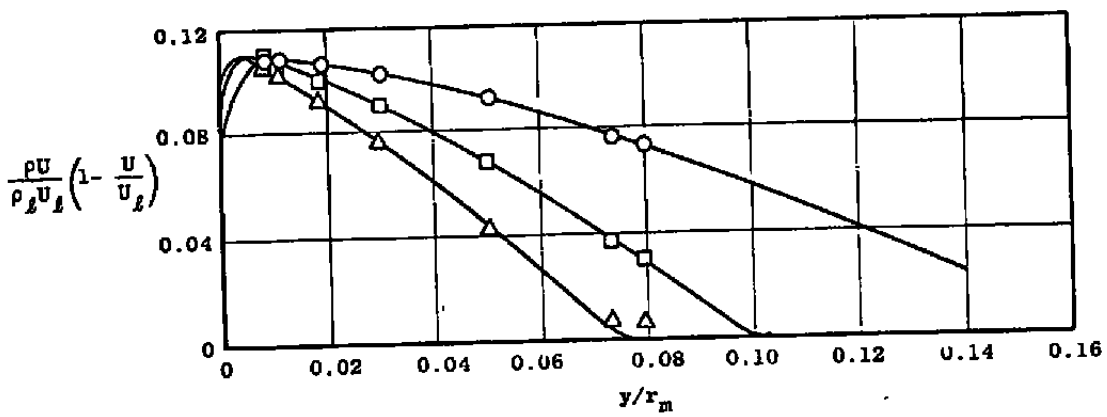

Momentum Profile

b. Re/in. = 0.84×10^6

Fig. 6 Concluded

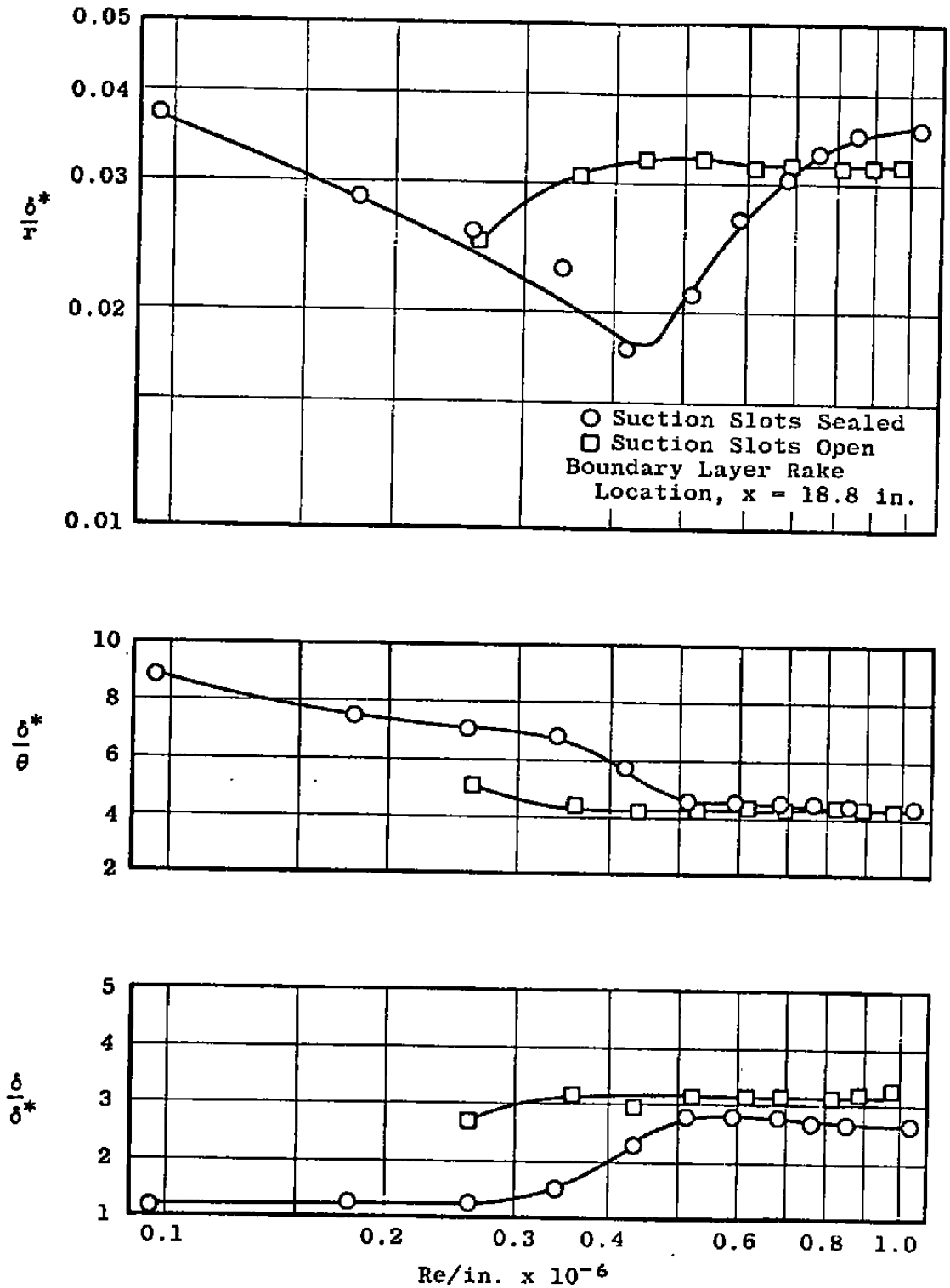

a. Mach Number 2.5

Fig. 7 Influence of Suction Slots on the Boundary-Layer Characteristics at Model Station 18.8 in.

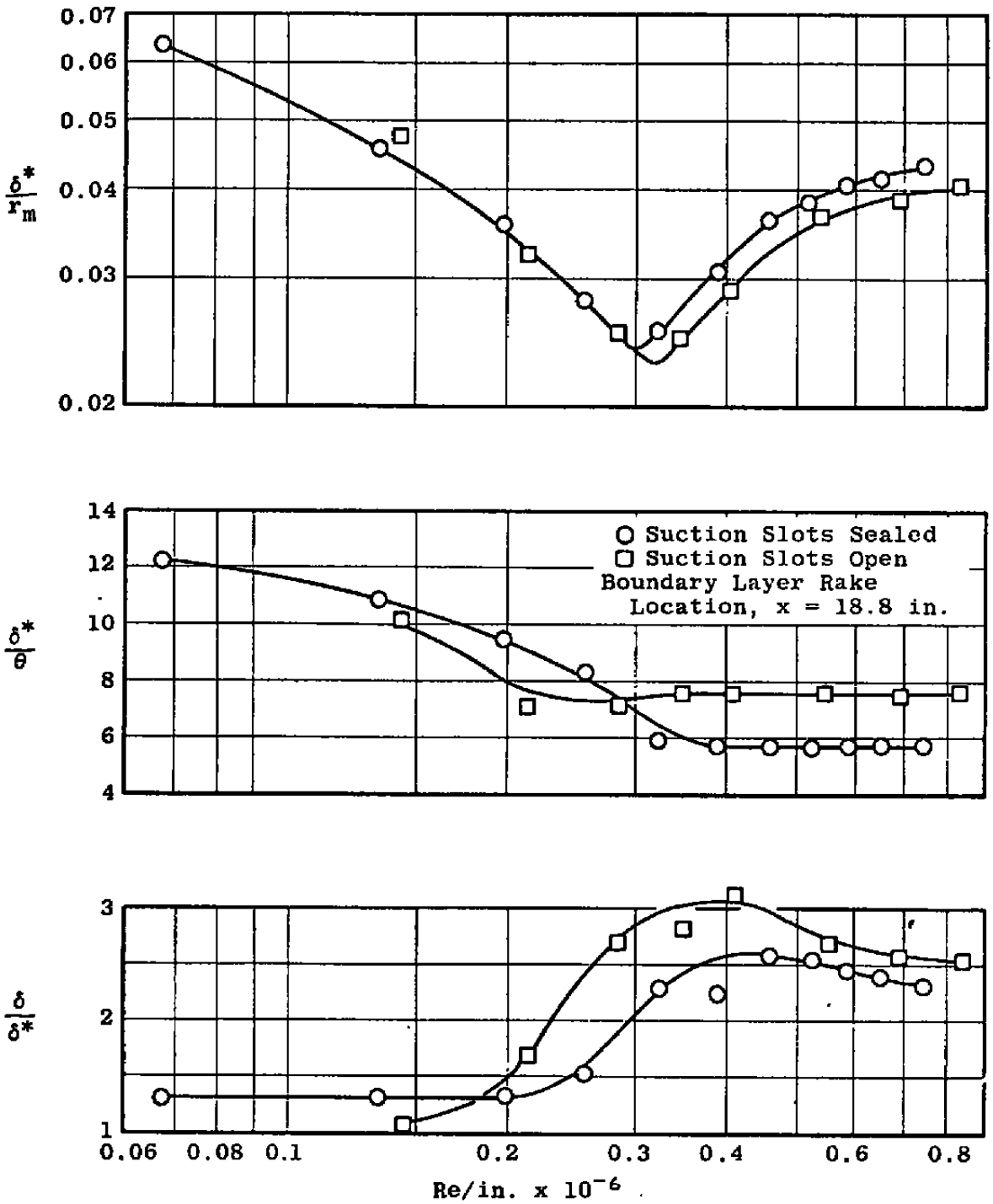

b. Mach Number 3.0

Fig. 7 Continued

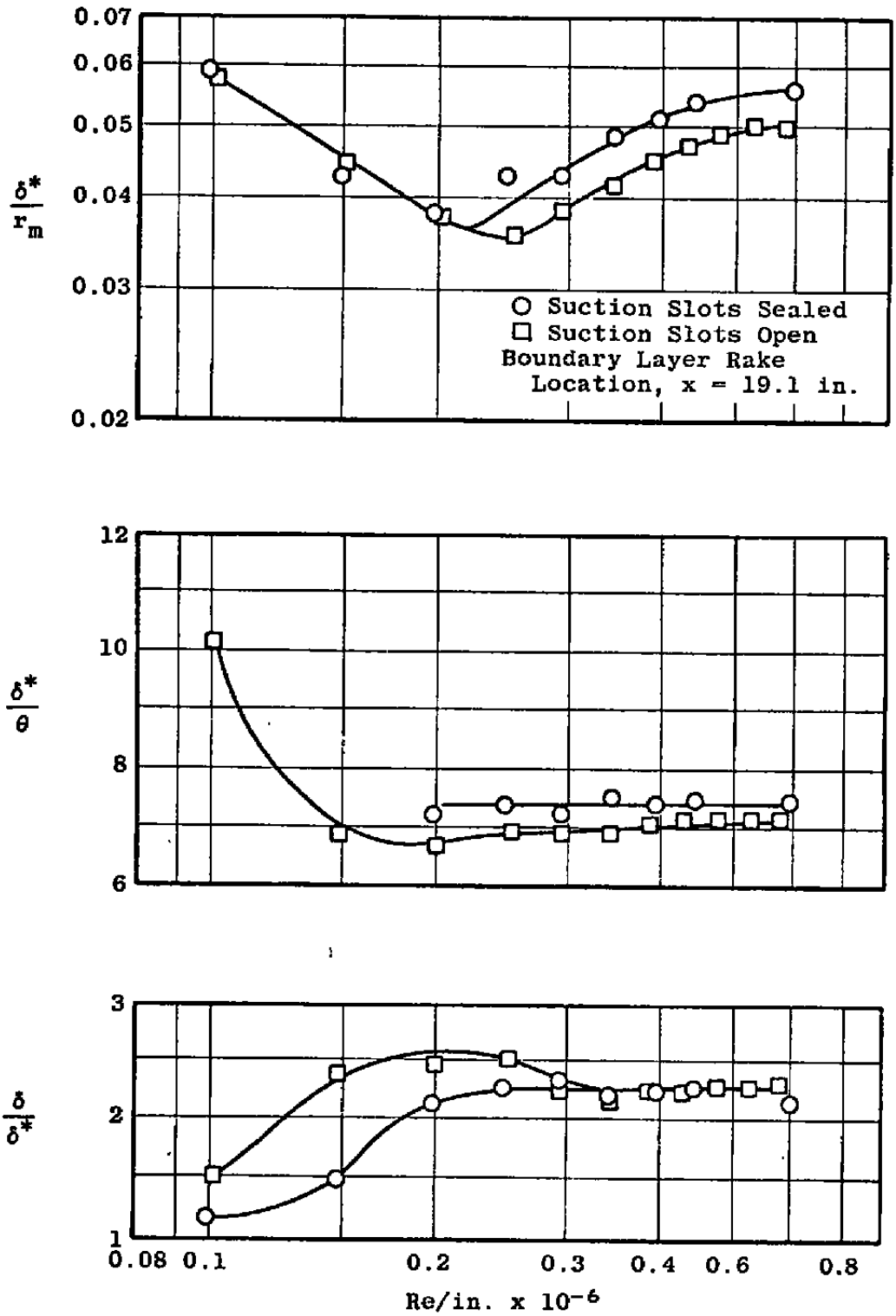

c. Mach Number 3.5

Fig. 7 Continued

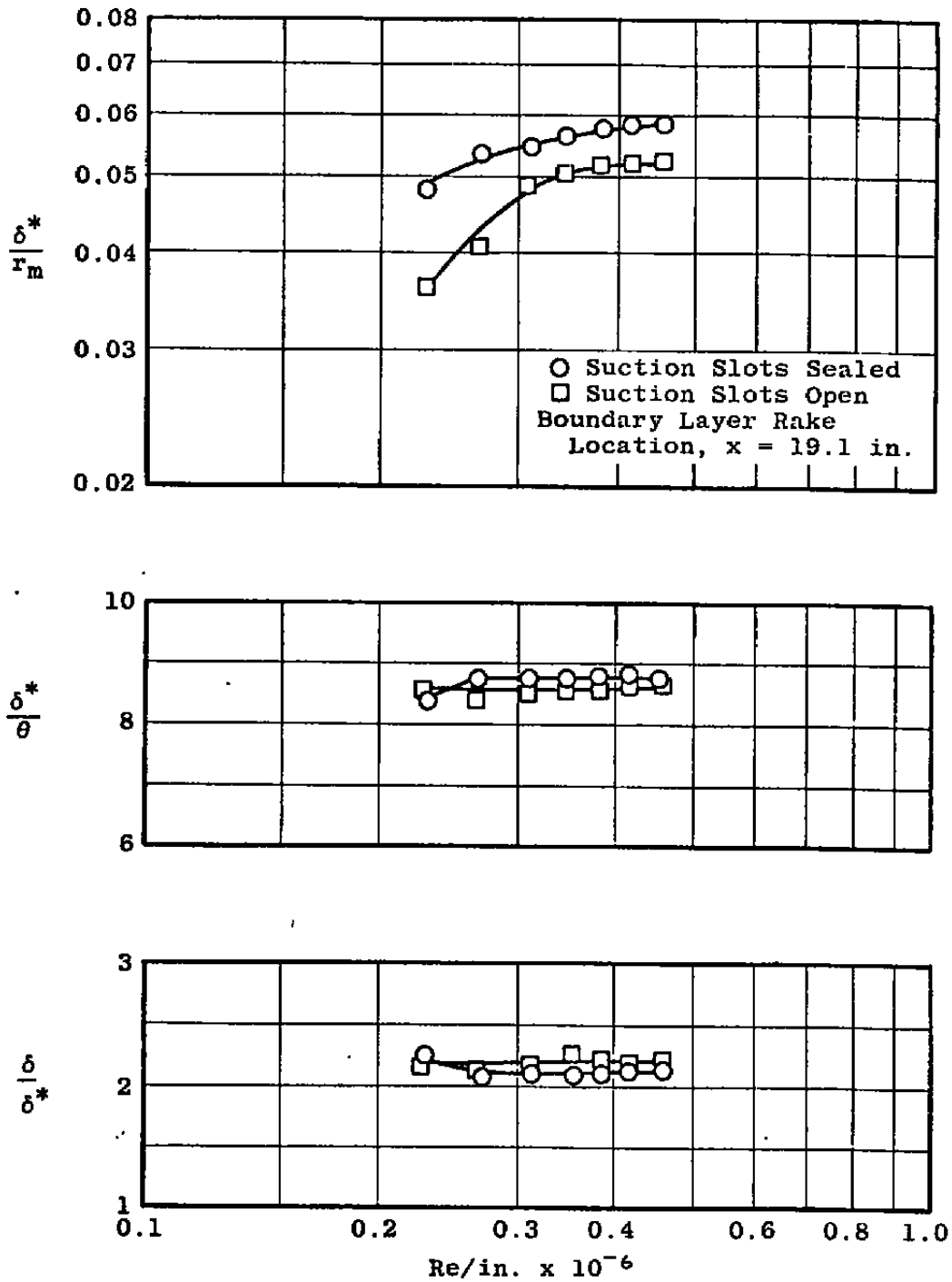

d. Mach Number 4.0

Fig. 7 Concluded

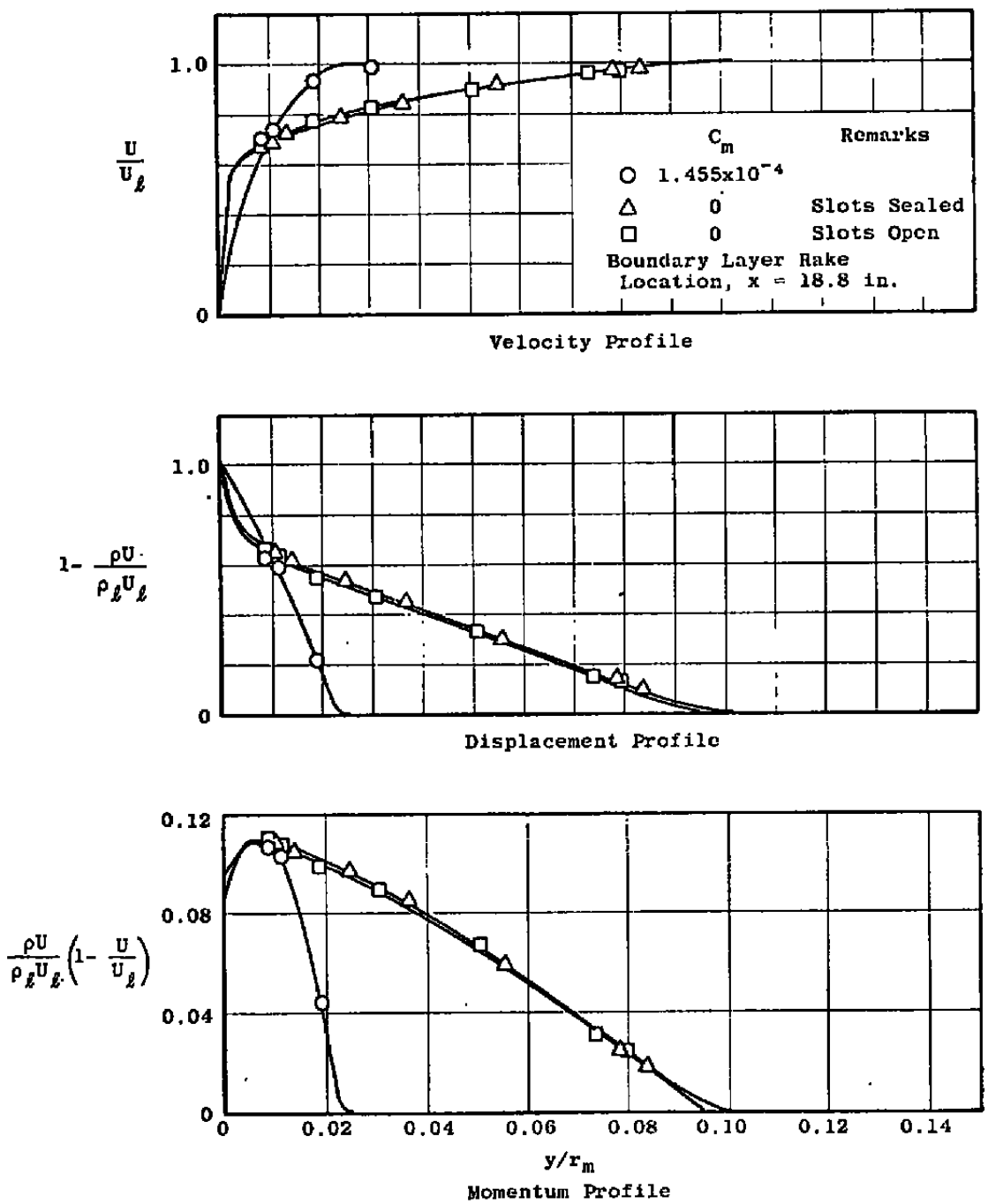

Fig. 8 Influence of Suction and Suction Slots on the Boundary-Layer Profiles at Mach Number 3, Ro/in. = 0.53 x 10^6

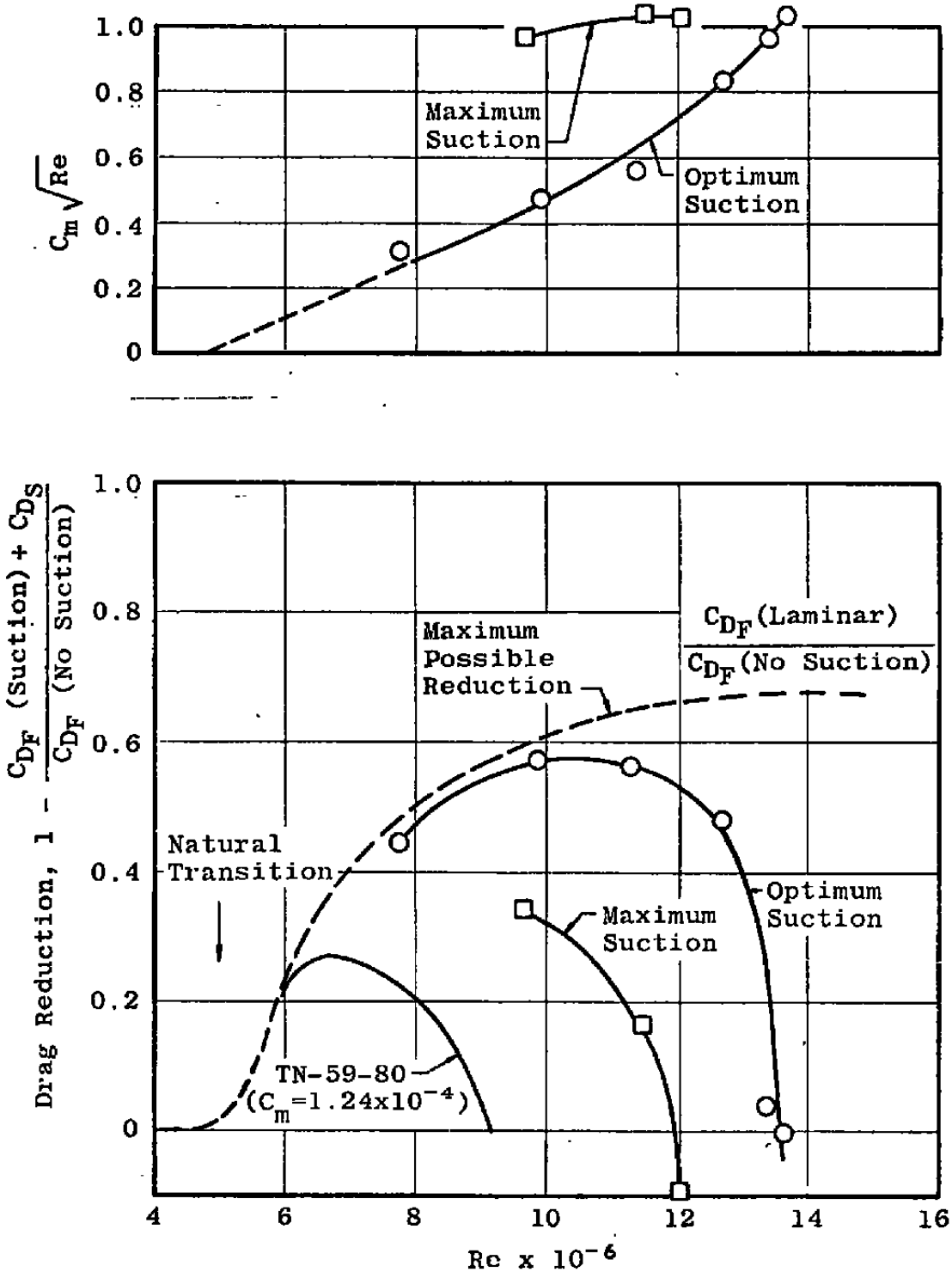

Fig. 9 Variation of the Optimum Suction and Drag Reduction with Reynolds Number at Mach Number 3

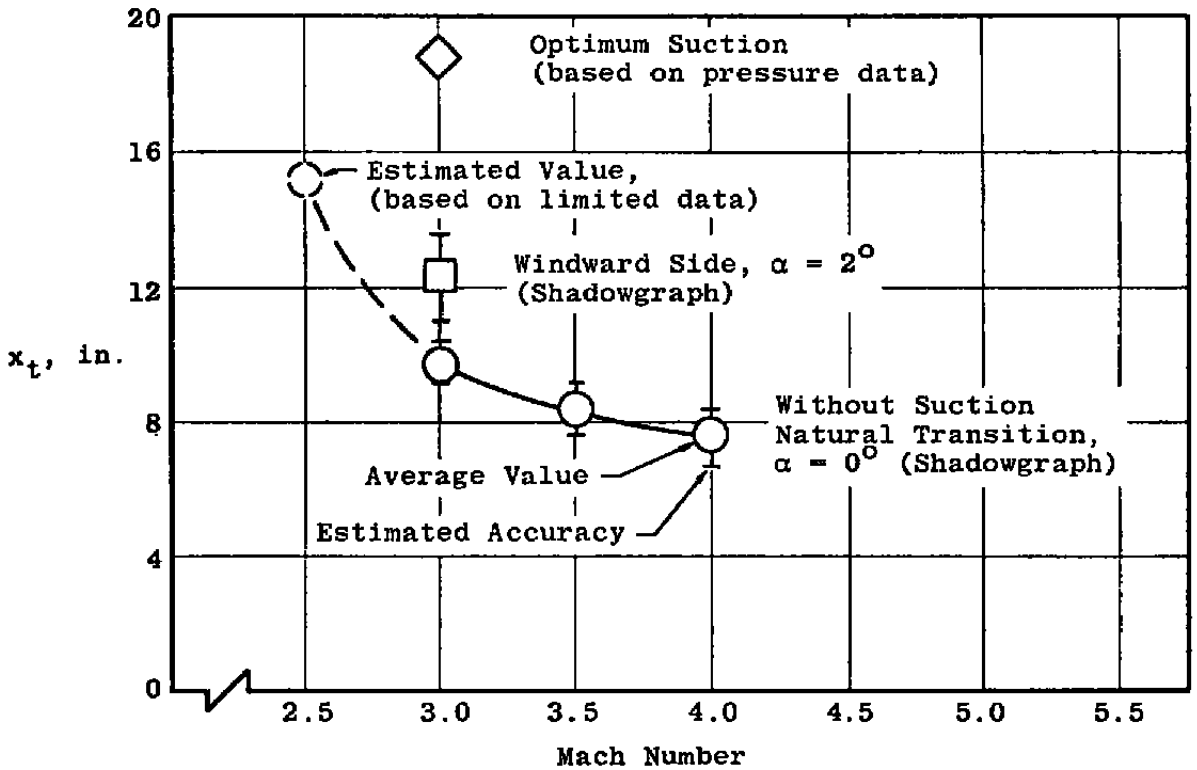

Fig. 10 Variation of Transition Location with Mach Number at Re/in. ≈ 0.53×10^6